Binding energies of hydrogen to the Si(111) 7×7 surface studied by statistical scanning tunneling microscopy

D. Rogers*

Department of Physics, University of British Columbia, Vancouver, British Columbia, Canada V6T 1Z1

T. Tiedje

*Department of Physics and Department of Electrical Engineering, University of British Columbia,
Vancouver, British Columbia, Canada V6T 1Z1*

(Received 21 July 1995)

The equilibrium distribution of hydrogen chemisorbed to adatoms on Si(111) 7×7 surfaces has been determined by counting the occupied adatom sites in scanning-tunneling-microscope images of hydrogen-treated Si surfaces. From the distribution of the chemisorbed hydrogen, we are able to determine the relative binding energies of hydrogen to the four different symmetry adatoms. [S0163-1829(96)51720-0]

Silicon surfaces are known to be highly reactive to atomic hydrogen. Hydrogen-treated silicon surfaces have been studied by various surface analysis techniques including electron-energy loss spectroscopy,[1] temperature programmed desorption,[2] low-energy electron diffraction (LEED)[2] and scanning tunneling microscopy (STM).[3,4] Of these techniques STM is uniquely capable of resolving individual surface atoms. In this paper we describe an STM study of the distribution of chemisorbed H on Si(111) 7×7 surfaces, following exposure to submonolayers of atomic H. Chemisorbed hydrogen is easily imaged by STM through its effect on the Si surface states. By a statistical analysis of STM images of H-treated Si surfaces, we show that it is possible to get remarkably precise information on the relative binding energies of H at different sites. Similar statistical STM techniques should be applicable to other chemisorption problems.

In these experiments, *p*-type Si(111) samples were prepared as follows: degrease in trichloroethylene, acetone, and methanol; etch in boiling nitric acid (70.5%) for 10 min, followed by 15 s in 2.5% hydrofluoric acid solution, and rinse in deionized water. The etching and rinsing steps were repeated three times followed by a final soak in boiling nitric acid for 10 min (to create a surface oxide) and then a rinse in deionized water. The sample was then loaded into a UHV chamber (2×10^{-10} Torr) through a load lock. Inside the UHV chamber the oxide and residual carbon were removed by heating the sample by direct resistive heating. The sample and its holder were outgassed by heating the sample to 550 °C for 12 h. Then the oxide was removed by heating to 850 °C for 10 min, and the carbon by heating to 1250 °C for 2 min.[5] The pressure was maintained in the 10^{-9} Torr range or less during the high-temperature anneal. The sample was cooled rapidly to 900 °C and then slowly (1 °C/s) to 550 °C and then allowed to cool to room temperature in about 2 h.

Above 550 °C the sample temperature was measured with an optical pyrometer. Below 550 °C, the temperature was inferred from a logarithmic extrapolation of the high-temperature measurements.[6] In this method the sample temperature T as a function of the heating current I is fit to the following relation:

$$\log_{10}T = a \log_{10}I + b, \tag{1}$$

in the temperature range from 598 to 867 °C, where $a = 0.280$, $b = 2.7758$, and T is measured in degrees Celius and I in amperes. The fit was then extrapolated to obtain the temperature at lower heating currents, below the range of the pyrometer calibration. Thermocouple calibrations below 550 °C on a test sample confirmed that Eq. (1) accurately describes the temperature for our sample configuration.

After the cleaning procedure described above, the surface exhibited a 7×7 LEED pattern, typical of the Si(111) 7×7 reconstructed surface, described by the dimer-adatom-stacking fault (DAS) model.[7] The 7×7 reconstruction was also seen by STM as shown in Fig. 1. The homebuilt STM is described elsewhere.[8] In this image, each 7×7 unit cell has two triangular arrays of six adatoms. We refer to the adatoms at the corners of the triangular arrays as corner adatoms and the adatoms in the middle as middle adatoms. The adatoms can also be distinguished according to whether they are on the faulted or unfaulted half of the unit cell. In STM images, at positive tip bias voltage, the adatoms on the faulted half of the surface unit cell appear brighter than the adatoms on the unfaulted side. Each adatom has one dangling bond that reacts readily with atomic hydrogen. In the DAS structure there are also six ''rest atoms'' per unit cell in the layer below the adatoms, which have dangling bonds that are not terminated by adatoms. The rest atoms can also be seen by STM, with positive tip bias, but are much less prominent than the adatoms. We have not attempted to image the rest atoms.

The Si surface was reacted with atomic H by exposing it to H_2 in the presence of a tungsten filament. The filament was located 15 mm in front of the sample and heated to 1900 °C, as measured with a disappearing filament pyrometer. To minimize radiative heating of the sample, exposure times were limited to 100 s. At the end of a 100 s exposure the sample temperature was found to increase slightly to 33 °C, as determined by a thermocouple mounted on a test sample. To ensure that there is no contamination of the sample by the filament, a test sample was placed close to the

<u>53</u>   R13 227

heated filament for 100 s with no hydrogen present. Afterwards, no changes were seen either in the LEED patterns or in the STM images.

From the filament geometry and the known dissociation rate of molecular hydrogen on hot tungsten we estimate that the flux of atomic H is 0.3% of the total molecular H_2 flux.[9] Hydrogen was introduced into the chamber at a pressure of 4.8×10^{-8} Torr and the filament heated for 100 s. This corresponds to an exposure of 4.8 L of H_2 or 0.01 L of atomic
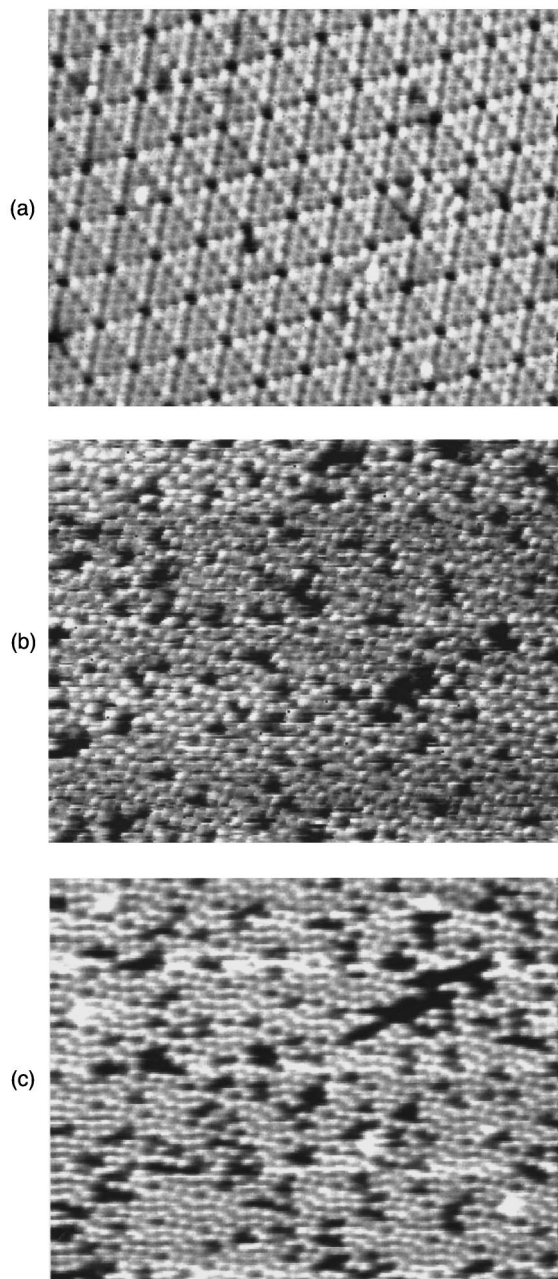
FIG. 1. STM images of Si(111) 7×7 surfaces: (a) Si surface prior to H exposure; (b) Si surface after exposure to 0.01 L of atomic H at an average temperature of 302 K; and (c) surface with the same H exposure as (b) followed by 735-K anneal for 20 s. The horizontal scan range in these images is 29 nm. The bias voltages on the tip were 2.5, −1.0, and −0.9 V for (a), (b), and (c), respectively. The tunneling currents were 1.8 nA, 2.4 nA, and 1.2 nA, respectively.

H. No change was observed in the LEED pattern for this exposure. Since the room temperature reactivity of Si with H_2 is more than six orders of magnitude lower than its reactivity with atomic H,[2] we assume that the H reaction stops when the filament is turned off. Figure 1(b) is an STM image of the surface, after this exposure, in which many of the adatoms appear to be missing. When a H atom bonds to an adatom, the surface states associated with the dangling bond are removed from the gap resulting in the apparent disappearance of the reacted adatom from the STM image.[3,4] Thus the adatoms that are missing in Fig. 1(b) are adatoms that have reacted with H. The apparent disappearance of some of the adatoms is not due to etching (removal) of the atoms: it has been shown that heating Si exposed to submonolayers of H up to the desorption temperature of the H does not etch the adatoms.[17]

By counting the reacted adatoms in STM images of H-exposed surfaces, we can determine the relative probabilities for H reactions with the four different adatoms sites. We counted the reacted adatoms in 2734 7×7 unit cells in 32 STM images similar to Fig. 1(b). For a total of 3850 reacted adatoms, we found that 1893 ± 31 or 49.2 ± 0.8 % were corner adatoms and 1957 ± 31 or 50.8 ± 0.8 % were middle adatoms. The error ranges are one standard deviation for a binomial distribution of 3850 events with a mean of 1957. There is a slight preference for reactions with the faulted half of the unit cell: 57.3 ± 0.8 % were on the faulted half and 42.7 ± 0.8 % were on the unfaulted half of the unit cell, with the statistical uncertainties calculated as before. Since we expect surface diffusion to be negligible at room temperature, we attribute the small asymmetry in the populations on the two halves of the unit cell to differences in the sticking coefficient.

After exposing the surface to 0.01 L of atomic H, we heated the sample at 658 K for total times of 20 s, 100 s, and 500 s. The thermal response time of the sample was found to be less than 1 s from thermocouple measurements. The H exposure was repeated on a fresh sample, which was subsequently annealed at 735 K for total times of 5 s, 20 s, 100 s, and 500 s. No changes were detected in the LEED patterns following the heat treatments; however, clear changes were observed in the STM images. A typical STM image of the surface after heating for 20 s at 735 K is shown in Fig. 1(c). As before, many of the adatoms are reacted with H, indicating that the heat treatment has not been severe enough to drive off the hydrogen. Similar images were obtained after the other heat treatments. Heating to 834 K was found to recover the complete 7×7 reconstruction, indicating that the H has been completely removed. This confirms that the Si adatoms that appeared to be missing were bonded to H and not removed by H etching.

The distribution of H on the different adatoms is shown in Figs. 2(a) and (b). This data was obtained from a number of different STM images before and after heat treatments at 658 K and 735 K. As shown in Fig. 2, H has a clear preference for the middle adatoms and for the faulted side of the unit cell after annealing. In Fig. 3 we show the total bonded H as a function of the annealing time at 658 K and 735 K, obtained from the same STM images. In Fig. 3 the percentage of reacted adatoms increases continuously with annealing time at 658 K. We attribute this increase to a net migra-
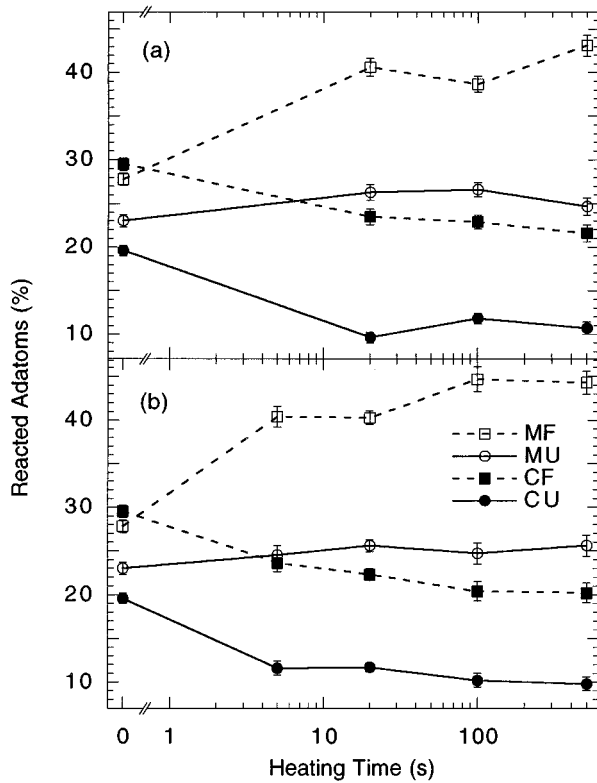
FIG. 2. Relative probability for H bonding to the four symmetrically distinct adatoms on Si(111) as a function of annealing time (a) at 658 K and (b) at 735 K. The adatoms are labeled by the letters C, M, F, and U, which mean ''corner,'' ''middle,'' ''faulted,'' and ''unfaulted'' respectively. The error bars are statistical uncertainties calculated from the number of atomic sites that were counted for each data point.

tion of H from the rest atoms to the adatoms. This suggests that H has a higher binding energy on the adatoms than on the rest atoms. At higher temperature (735 K) the percentage of reacted adatoms increases, then decreases, with annealing time. The initial increase is believed to be due to migration of H from the rest atoms to the adatoms, as observed with the 658-K annealing. The longer-term decrease is due to loss of H by evaporation.
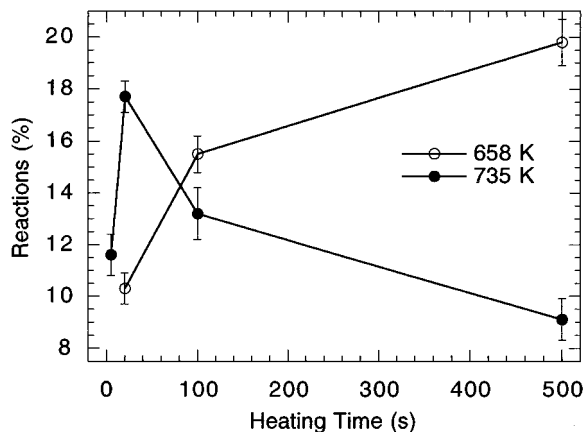

FIG. 3. Fraction of Si adatoms with chemisorbed H as a function of annealing time at 658 K and 735 K.

The H-atom distributions observed by STM at room temperature were found to be unchanged over times differing on the order of hours (2–7 h) from the time of the heat treatments. This is reasonable given the expected 1.5-eV activation energy for H diffusion.[10] If the attempt frequency is 10^{12} s^{-1} and the activation energy is 1.5 eV then at 735 K the hop time for hydrogen will be about 20 ms. In this case the room-temperature hop time is orders of magnitude longer than the experimental time scale.

With sufficiently high annealing temperature and enough time, the hydrogen distribution will achieve an equilibrium among the different chemisorption sites. Referring to Fig. 2(b), since the distribution is unchanged following the 100-s anneal at 735 K, we conclude that this is an equilibrium distribution.

From this equilibrium distribution, we can infer the relative binding energies of H at the different sites. In thermal equilibrium the probability p_i that a hydrogen atom is bonded to a site with binding energy E_i is

$$p_i = \frac{1}{Z} \exp\left(-\frac{E_i}{kT}\right), \qquad (2)$$

where Z is the partition function, k is Boltzmann's constant, and T is the temperature. To obtain the probabilities in thermal equilibrium, the data for the 100 s and 500 s heat treatments at 735 K are averaged resulting in $p_{cu}=0.100\pm0.006$, $p_{cf}=0.203\pm0.008$, $p_{mu}=0.252\pm0.008$, and $p_{mf}=0.445\pm0.010$, where c and m refer to corner and middle adatoms, respectively, and u and f refer to adatoms on the unfaulted and faulted half of the unit cell, respectively. These results were compiled from 23 STM images by counting 2619 reacted adatoms in 2049 7×7 unit cells. The statistical errors were calculated as before. From Eq. (2) and the thermal equilibrium probabilities, we find that the relative binding energies of the four different symmetry adatom
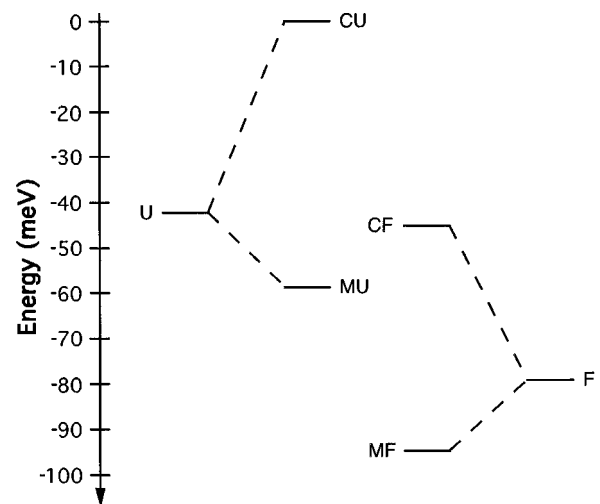

FIG. 4. Energy-level diagram showing the relative binding energies for H on the adatoms located at the corner and middle sites on the faulted and unfaulted sides of the 7×7 unit cell. The lines marked U and F indicate the average binding energy for the equilibrium population of H on the faulted and unfaulted sides of the Si(111) 7×7 surface unit cell.

sites on the Si(111) surface are $E_{cu}-E_{cf}=44.8\pm6.3$ meV, $E_{cu}-E_{mu}=58.5\pm5.8$ meV and $E_{cu}-E_{mf}=94.5\pm5.2$ meV. The results are shown schematically in the energy-level diagram in Fig. 4.

This analysis assumes that the sample cooling is sufficiently fast that the hydrogen equilibrium is not representative of a lower-temperature freeze-in point during the cooldown. The equilibrium distribution is unlikely to change much during the cooldown in our experiment for the following reasons. First, the sample heated for 5 s has a different hydrogen distribution than the ones that are heated for longer times, which suggests that 5 s is not enough for full equilibration to take place. This means the equilibrium population is established during the high-temperature anneal and not during the cooldown. Secondly the diffusion of hydrogen is much more strongly temperature dependent than the equilibrium population distribution among the various sites. This means the H diffusion rate will change drastically with a much smaller change in the equilibrium population during the cooldown.

As shown in Fig. 4, the average binding energy for hydrogen on the faulted side of the unit cell is 37 meV larger than on the unfaulted side of the unit cell. This is consistent with electronic structure calculations, which show that the adatom dangling bond band is 70 ± 70 meV more strongly bound on a faulted Si(111) crystal surface than on an unfaulted surface.[11] Also, STM studies of Pd,[12] Li[13] and C_6H_5Cl (Ref. 14) on Si(111) show preferential bonding to the faulted part of the unit cell. There are no electronic structure calculations of the surface-state energies for the corner and middle adatoms. However the corner adatoms are bonded to three first-layer Si atoms that are all bonded to Si dimers in the layer below. In the case of the middle adatoms, on the other hand, only two of the three first-layer atoms below the adatoms are bonded to Si dimers. Thus the second-neighbor interactions are different and could be responsible for the observed differences in the binding of hydrogen to the middle and corner adatoms. Second-neighbor overlap integrals are on the order of 100 meV in silicon.[15] This is the same order as the difference in the middle and corner adatom binding energies for hydrogen. STM studies of ammonia adsorption on Si(111) 7×7 also show preferential adsorption on the middle adatoms.[16]

By extending the statistical analysis of the H distribution to lower temperatures one may be able to explore the approach to thermal equilibrium and obtain atomic scale information about the kinetics of H diffusion on Si surfaces in addition to the equilibrium information.

In conclusion, we have measured the thermal equilibrium distribution of chemisorbed H on Si(111) 7×7 surfaces from a statistical analysis of STM images. From the measured distribution we are able to infer the relative binding energies of H on the four symmetrically distinct adatom sites on the Si(111) 7×7 surface.

*Present address: Chemistry Department, University of Toronto, Toronto, Ontario, M5S 1A1.

[1] H. Kobayashi, K. Edamoto, M. Onchi, and M. Nishijima, J. Chem. Phys. **78**, 7429 (1983).

[2] G. Schulze and M. Henzler, Surf. Sci. **124**, 336 (1983).

[3] K. Mortensen, D. M Chen, P. J. Bedrossian, J. A. Golovchenko, and F. Besenbacher, Phys. Rev. B **43**, 1816 (1991).

[4] J. J. Boland, Surf. Sci. **244**, 1 (1991).

[5] B. S. Swartzentruber, Y.-W. Mo, M. B. Webb, and M. G. Lagally, J. Vac. Sci. Technol. A **7**, 2901 (1989).

[6] S. Hasegawa, Y. Nagai, T. Oonishi, and S. Ino, Phys. Rev. B **47**, 9903 (1993).

[7] K. Takayanagi, Y. Tanishiro, S. Takahashi, and M. Takahashi, Surf. Sci. **164**, 367 (1985).

[8] D. Rogers and T. Tiedje, Surf. Sci. Lett. **274**, L599 (1992).

[9] J. N. Smith and W. L. Fite, J. Chem. Phys. **37**, 898 (1962).

[10] G. A. Reider, U. Hofer, and T. F. Heinz, Phys. Rev. Lett. **66**, 1994 (1991).

[11] R. D. Meade and D. Vanderbilt, Phys. Rev. B **40**, 3905 (1989).

[12] U. K. Kohler, J. E. Demuth, and R. J. Hamers, Phys. Rev. Lett. **60**, 2499 (1988).

[13] Y. Hasegawa, H. Tochihara, M. Kubota, and Y. Murata, J. Vac. Sci. Technol. A **8**, 238 (1990).

[14] X. H. Chen, Q. Kong, J. C. Polanyi, D. Rogers, and S. So, Surf. Sci. **340**, 224 (1995).

[15] D. A. Papaconstantopoulos, *Handbook of the Band Structure of Elemental Solids* (Plenum, New York, 1986).

[16] R. Wolkow and Ph. Avouris, Phys. Rev. Lett. **60**, 1049 (1988); Phys. Rev. B **39**, 5091 (1989).

[17] T. Sakurai, Y. Hasegawa, T. Hashizume, I. Kamiya, T. Ide, I. Sumita, H. W. Pickering, and S. Hyodo, J. Vac. Sci. Technol. A **8**, 259 (1990).